ORIGINAL RESEARCH ARTICLE

Determination of the Partial Contributions to the Electrical Conductivity of TiO$_2$-SiO$_2$-Al$_2$O$_3$-MgO-CaO Slags: Role of the Experimental Processing Conditions

SAMUEL MARTIN-TRECENO, ANTOINE ALLANORE, CATHERINE M. BISHOP, MATTHEW J. WATSON, and AARON T. MARSHALL

The electrical transport properties of molten TiO$_2$–SiO$_2$–Al$_2$O$_3$–MgO–CaO slags were determined as a function of temperature and oxygen partial pressure. To avoid the corrosion of crucible materials by this slag at ultra high temperatures, the pendant droplet technique was used inside a modified floating zone furnace. Electronic and ionic transference numbers were estimated using stepped-potential chronoamperometry experiments to quantify the contribution of the electronic/ionic conductivity to the total electric conductivity. The results show that these slags are mixed conductors, where current is carried by ionic and electronic carriers. The oxygen partial pressure dependence of the electronic transference numbers, t_e, indicated a semiconducting mechanism in the molten slag. The ratio of the different valences of the transition metal ions had a predominant effect on the t_e. The TiO$_2$ content also favoured electronic conduction, while the effect of temperature and structure was less noticeable within the temperature and composition range studied.

I. INTRODUCTION

THE use of molten oxide electrolysis (MOE) to produce metals has been proven more sustainable and environmentally friendly than the common, carbon-intensive, traditional metallurgical processes.[1] The potential to reduce emissions to the environment increases if large-scale waste materials are used as feedstock for this process. Along these lines, previous work[2] has shown that the electrochemical recovery of metals from molten TiO$_2$−SiO$_2$$s$−Al$_2O_3$−MgO−CaO slag, a by-product of some ironmaking processes, is feasible, although the process had very low faradaic efficiency. Moreover, Ti-bearing slag has been proposed as a substitute for rutile as the feedstock for the titanium industry.[3] However, a more extensive understanding of the electrical properties of this complex oxide system in its molten state is paramount in the design of industrial electrochemical cells.[4]

Knowledge about the electrical resistivity of the melt is essential to establish the thermal balance of the electrochemical cell,[5] as the ohmic drop affects the cell voltage of the electrochemical reaction of interest[6] and is one of the major sources of heat generation in a high temperature electrolysis reactor.[7] To simulate a process where titanium is continuously extracted from the slag, the determination of the variability of specific electrical conductance or total electrical conductivity (σ, S cm^{-1}) with TiO$_2$ concentration is necessary. For TiO$_2$-SiO$_2$-Al$_2$O$_3$-MgO-CaO slags, it has been found to vary from 0.2 to 2 S cm^{-1} with concentrations up to 30 wt pct TiO$_2$.[8,10] This value keeps increasing as the concentration of TiO$_2$ increases, with Hu et $al.$[3] reporting values up to 141 S cm^{-1} for molten TiO$_2$-Ti$_2$O$_3$-FeO-SiO$_2$-Al$_2$O$_3$-MgO-CaO slags with a high titania content.

SAMUEL MARTIN-TRECENO, AARON T. MARSHALL, and MATTHEW J. WATSON are with the Department of Chemical and Process Engineering, University of Canterbury, Christchurch 8140, New Zealand. Contact e-mail: aaron.marshall@canterbury.ac.nz ANTOINE ALLANORE is with the Department of Materials Science and Engineering, Massachusetts Institute of Technology, Cambridge, MA 02139. CATHERINE M. BISHOP is with the Department of Mechanical Engineering, University of Canterbury, Christchurch 8140, New Zealand. AARON T. MARSHALL and CATHERINE M. BISHOP are with the MacDiarmid Institute of Advanced Materials and Nanotechnology, Christchurch 8140, New Zealand.

In molten oxide electrolytes the current is transported through the melt by both ionic and electronic charge carriers,[3,11–13] and, consequently, the charge transport mechanism across the electrolyte defines how much of the applied current is used in the reaction of interest. Transference numbers quantify the contribution of each charge carrier.[12] Fried et al.[11] proposed a framework to perform transference number measurements in a molten $TiO_2 - BaO$ mixture, but their study was limited to a narrow range of compositions and to temperatures below those required for the electrolysis of molten slag. In MOE is of particular importance to understand the role of the process parameters in the conduction mechanism as it helps to determine the current efficiency of the electrolysis.

The purpose of the present study is to quantify the contribution of the ionic and electronic charge carriers in the electrolysis of TiO_2-SiO_2-Al_2O_3-MgO-CaO slags. Here, transference number measurements are performed to determine to what extent the conductive mechanism is affected by changing the experimental processing conditions, such as temperature, oxygen partial pressure and electrolyte composition. Transference numbers are obtained using stepped-potential chronoamperometry (SPC), and their contribution to the mixed conduction mechanism in the molten slag is discussed.

II. EXPERIMENTAL METHODS

A. Sample Preparation

Reagent grade TiO_2 (99.9 pct, CERAC Inc.), SiO_2 (99.4 pct, CARLO ERBA Reagents), Al_2O_3 (98 pct, CARLO ERBA Reagents), $(MgCO_3)_4 \cdot Mg(OH)_2 \cdot 5H_2O$ (99 pct, SIGMA-ALDRICH), and $CaCO_3$ (99.95 pct, CERAC Inc.) powders were used as starting materials to prepare three compositions of a synthetic TiO_2-SiO_2-Al_2O_3-MgO-CaO slag. The compositions studied in this paper are representative of Ti-bearing slag formed in the ironmaking process in New Zealand. The TiO_2 concentration has been lowered, while keeping the relative amounts of the other oxides approximately constant, to simulate a process where only titanium is continuously extracted from the slag. X-ray fluorescence spectroscopy (XRF, Siemens/Bruker SRS3000) was used to measure the compositions of the samples (Table I). The steps to prepare the final, rod-shape samples used in the furnace have been described before.[2]

B. Electrochemical Measurements and Operation

In this work, all the electrochemical measurements were carried out by contacting a pendant droplet of molten slag with electrodes inside a modified thermal imaging furnace (TX-12000-I-MIT-VPO-PC, Crystal Systems Corp.). This containerless technique and the details regarding the assembly of the electrodes and electrical connections to the potentiostat, have been described before.[2,15] Briefly, the sintered sample was suspended from the upper furnace shaft inside a quartz tube, while the electrode probe was inserted through the bottom port. Their position was adjusted using two individual stepper motors with

submillimeter precision. Real time visualization during experimentation was achieved through a flat window in the quartz tube using a camera (EOS Rebel T5i DSLR, Canon Inc.) with a telescopic lens.

At the beginning of each experiment, the electrochemical cell was purged three times before turning on the furnace. Argon gas (UHP 99.999 pct, 50 ppm O_2 or 100 ppm O_2; Airgas Inc.) at a flow rate of 200 mL min^{-1} was used to refill the chamber and during operation. The molten droplet was contacted with a type C thermocouple (W-Re (5 wt pct) | W-Re (26 wt pct)) to determine the operating temperature with $\pm$ 1 pct maximum error. Once the operating temperature (i.e., furnace lamp power) was chosen, the pendant droplet was formed by lowering the sample until its bottom end was in the hot zone. At the hot zone, the sample was rotated until the pendant droplet was stable. Then, the electrodes were raised into the molten droplet to an immersion depth of approximately 2 mm. A sudden change in the open circuit potential (OCP), alongside the in situ visualization, confirmed that the electrodes had contacted the molten droplet.

For all measurements, a three-electrode configuration held inside an Al_2O_3 four-bore tube was used. The working (WE), counter (CE) and pseudo-reference electrode (REF) consisted of individual metallic wires immersed into the molten slag droplet. This type of reference electrode can provide a stable potential,[16] and it is commonly used in MOE. Iridium (Ir > 99.9 pct, diameter = 0.5 mm, Furuya Metals Co., Ltd.) was chosen as the electrode material due to its high melting point and mechanical stiffness. Both properties are required to repeatedly insert thin electrode wires into the molten slag. Moreover, Ir does not react with the slag or oxidise under the experimental conditions,[2] and has been successfully used as electrodes in the electrolysis of molten oxides before.[2,15,17]

All the electrochemical measurements were conducted using a potentiostat (Gamry Reference 3000). Each measurement began by recording the OCP. The ohmic resistance of the electrolyte (R_{slag}) between the working and pseudo-reference electrode was calculated from electrochemical impedance spectroscopy (EIS) measurements at OCP, using an AC amplitude of 10 mV over a frequency range of 100 kHz to 1 Hz (10 points/decade). Transference number measurements were obtained using SPC to quantify the fraction of the charge carried by ionic (anions and cations) or electronic (electrons and holes) carriers. Temperatures in the vicinity of T_{liq} were chosen, ranging from 1773 K to 1933 K. The working electrode was maintained at OCP for 15 seconds before being stepped to 0.01 V vs OCP for 30 seconds (Figure 1). Cyclic voltammetry confirmed that the SPC measurements were within a potential window where no faradaic reactions occurred.

C. Considerations and Measurement Principles

1. Phase Relations

The phase relations were required to study the slags at temperatures in the vicinity of T_{liq}. For each slag composition, at a total pressure of 1 atm, the phase relations were predicted as a function of temperature

Table I. Electrolyte Compositions (Wt Pct) Measured by XRF in Ascending Order of Their Predicted Liquidus Temperature, T_{liq}. Predicted Solidus Temperature, T_{sol}, and Optical Basicity, Λ_{corr}, Calculated According to Ref. 14 are Given

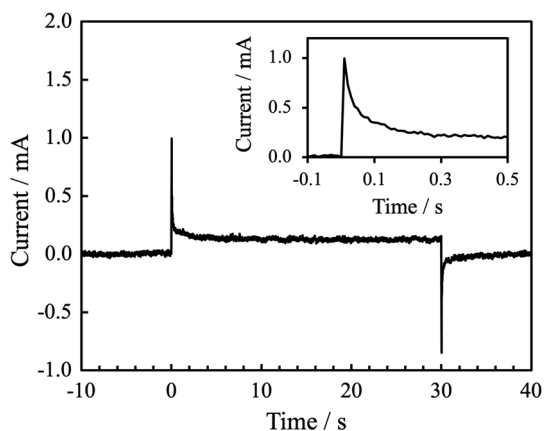|	TiO_2 Wt Pct	CaO Wt Pct	SiO_2 Wt Pct	Al_2O_3 Wt Pct	MgO Wt Pct	Λ_{corr} —	T_{sol} K	T_{liq} K
Slag A	33	18	15	19	15	0.629	1486	1803
Slag B	15	24	25	18	18	0.635	1494	1823
Slag C	9	25	26	20	19	0.633	1494	1883

Fig. 1—Current *vs* time response for Slag B at 1933 K following a potential step from OCP to 0.01 V *vs* OCP (at t = 0 s) then back to OCP (at t = 30 s). Inset: magnified view of the short time current decay.
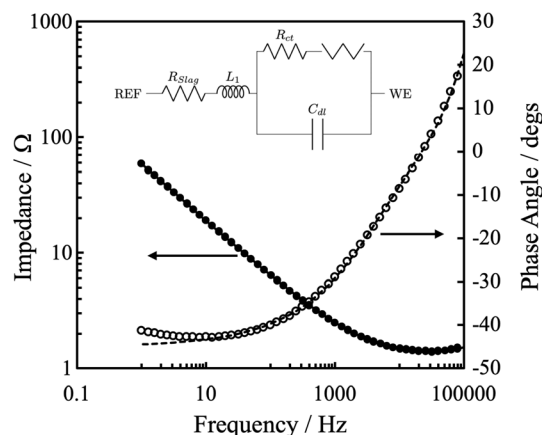

Fig. 2—Bode plot recorded at OCP for Slag C at 1903 K (10 mV excitation, 100 kHz to 1 Hz). The experimental data are represented with points while a line is used for the fitted model. Insert: equivalent circuit diagram used to model impedance measurements in this study.

using the thermodynamic software FactSage 7.2.[18] Model parameters are from FToxid and FactPS databases. The solidus temperature (T_{sol}), minimum temperature for any liquid phase to be stable, and the T_{liq}, maximum temperature for any solid phase to be stable, were determined. These values are reported in Table I, and were calculated for $P_{O_2} = 10^{-6}$ atm. These predictions have been validated using differential scanning calorimetry (DSC) and *in situ*, high temperature X-ray powder diffraction (XRD) techniques in previous work.[2]

2. Electrolyte Resistance

EIS measurements were used to measure the total resistance between the working and pseudo-reference electrode. A typical impedance spectrum recorded at OCP for Slag C at 1903 K is presented in Figure 2. A modified Randle's circuit (Figure 2 insert) was used to fit the impedance spectra based on previous work.[17] The inductive element, L1, is associated with the long electrode leads between the cell and potentiostat when using this furnace for ultra-high temperature electrochemical measurements.[17]

Typical R_{slag} values for the experiments ranged from 1 to 3 Ω, and overall, the electrolyte resistance varied with the slag composition, the atmosphere used, and electrode configuration (*i.e.,* size of working electrode, and its distance to the pseudo-reference electrode[19]). In this

work, the distance between both electrodes was approximately 2 mm and the area of the working electrode was 0.035 cm². The ohmic contributions from the lead wire (at room temperature) and electrode wire itself (at the operating temperature[20]) was estimated to be approximately 0.3 Ω. While we attempted to maintain a constant electrode immersion depth into the molten droplet, it was found that the oxide composition and oxygen partial pressure influenced the wettability of the Ir electrodes by the molten oxide, which meant that between measurements of different oxide composition or oxide partial pressures, the exact immersion depth could not be controlled. This means that the cell constant required to calculate the electrolyte resistivity from EIS measurements could not be determined. This limits the EIS data to revealing how the resistance between the working and reference electrode changed as a function of temperature.

The effect of the electrolyte resistance in fast transient electrochemical measurements must be taken into account.[19] In SPC measurements the potential step must be applied to the electrode rapidly by the potentiostat, with the cell time constant controlling the time domain over which the distortion to the potential applied to the cell is significant. For systems where no faradaic reactions occur at the potential applied to the cell, the time constant is defined by the charging time of the double-layer, $R_{slag}C_{dl}$, where C_{dl} is the double-layer capacitance. The associated current will drop to

virtually zero after a time equivalent to a few time constants.[19] For the electrode geometries used in this work, the time associated with double-layer charging is in the range of 10^{-5}-10^{-6} seconds, which is consistent with reports for molten oxides.[11,17] The experiments were designed to minimize its effect by choosing a time scale on the order of seconds for the experiments, and a resolution time of 10 milliseconds to accurately capture the current response to the potential step.

3. Ionic and Electronic Charge Carrier Contribution

While EIS is often used to measure the ohmic resistance of electrolytes across aqueous and non-aqueous media, there is no standardised technique to measure transference numbers in corrosive, ultra-high melting temperature electrolytes such as the $TiO_2-SiO_2-Al_2O_3-MgO-CaO$ slag. Olsen et al.[21] reviewed different experimental methods for measuring transference numbers, such as nuclear magnetic resonance and Radio Tracer, Hittorf, ac-impedance, dc-polarization (i.e., SPC) and the concentration cell. They concluded that the predominant Hittorf method is as effective as the SPC for the determination of transference numbers if the ion pairs, i.e., electron donor/acceptor couples, are present and mobile. Prior literature on molten oxides suggests that these conditions are met.[12,22] SPC is normally chosen over the Hittorf method, as the latter method is technically difficult to conduct at the ultra-high temperatures required for molten oxide systems. The SPC method been used previously for measuring transport properties of oxide melts,[6,7,11,12] sulfide melts,[23] salts,[24] and even solid oxide electrolytes and polymers.[21]

The transference numbers obtained using this technique are always positive*, and express how charge is

---

*The sign of transference numbers calculated from SPC technique do not reflect the direction of transport. These transference numbers are called internal as they are referred to a fixed amount of a compound or ion.[24]

---

carried across the electrolyte. In a mixed conductor, the ionic transference number, t_i, is the fraction of the current that is carried by ionic charge carriers. The contribution of the electronic charge carriers is referred to as the electronic transference number, t_e. Both contributions sum to unity:

$$t_i + t_e = \frac{I_i}{I_t} + \frac{I_e}{I_t} = 1 \qquad [1]$$

where I_i is the current carried by ionic charge carriers, I_e is the current carried by electronic charge carriers, and I_t is the total electric current. Provided the charge carriers are distributed homogeneously in the melt, i.e., a homogeneous electric field is present, the partial contributions to the total electrical conductivity can be calculated from the corresponding transference numbers as:

$$\sigma_{i/e} = \sigma \cdot t_{i/e} \qquad [2]$$

Fried et al.[11] showed this technique is capable of differentiating between the ionic and electronic conductivity

(σ_i and σ_e, S cm^{-1}) in titanate melts. They modelled the charge transport dynamics in the bulk melt originating as a response to an electric field (stepped-potential) for a system with mixed conduction. Based on the assumption of quasi-neutrality in an imposed field model, if there are no faradaic reactions occurring at the potential applied, the dynamics in the bulk melt result from the current due to the diffusion of ions and ohmic conduction. The model isolates the charge transport dynamics in the bulk by defining time limits that exclude dynamics arising from the electrode processes and external circuit elements, as well as any bounding double layers (migration and concentration gradients). On this time scale it is demonstrated that, if the cell time constant for the system under study is small compared to the time scale of the experiment, there is no net charge accumulation in the bulk, and the current in the bulk is merely ohmic. Hence, the material in the bulk will remain uncharged, sustaining the quasi-neutrality assumption. This approach was validated for this work by comparing the cell time constant (microseconds, discussed in the previous section) to the time scale of the charge transport dynamics in the bulk (seconds). A limitation of the technique is that it cannot distinguish which ion is the charge carrier if there are a plurality of mobile ionic species, nor the electronic charge carrier.

Transference numbers can be calculated by monitoring the current response to a potential step as a function of time (Figure 1). After the potential is applied, the current decay as a function of time can be correlated to the transition from mixed to pure electronic conduction. Consequently, the t_e can be calculated from the value of the two limiting cases, the initial current peak and the value at the long time limit:

$$t_e = \frac{I_{t\to\infty}}{I_{t\to 0}} \qquad [3]$$

When the potential step occurs, there is a uniform concentration of ions outside of the double layer, and $I_{t\to 0}$ is purely ohmic (ion + electron drift). At the long time limit, $t \to \infty$, the ion concentration will no longer be uniform. However, since no faradaic reactions are occurring at the electrodes, diffusion balances drift, and $I_{t\to\infty}$ is, again, solely ohmic (only electron drift). To exclude the double-layer charging current, times $> 3R_{slag}C_{dl}$ must be chosen as the short time limit. Here, as the data were acquired at 100 Hz, the short time limit ($t \to 0$) was selected as $t = 10$ ms. This conservative approach will likely overestimate the calculated electronic transference number compared but ensures that the current will be essentially free from double-layer charging effects.[19]

III. RESULTS AND DISCUSSION

A. Conductive Mechanism

Molten metal oxide electrolytes are proven mixed conductors, where current is conducted by ionic and electronic carriers.[12] Here the mixed conductivity of molten $TiO_2-SiO_2-Al_2O_3-MgO-CaO$ slags is

investigated using SPC measurements (Figure 1), with the behaviour of the current transient agreeing well with reported SPC measurements previously reported for titanate melts.[11] The electronic contribution is illustrated by the non-zero value of $I_{t \to \infty}$. As discussed in the previous section, any current present at $t \to \infty$ is representative of electronic conduction.

In molten transition metal oxide bearing slags, pure electronic charge transfer, as reported for solid glasses,[25] is an unlikely mechanism for the electronic conduction. "Free" electrons in the melt are instead attracted to the 3d-orbitals of the transition metals cations.[25] Mott[26] interpreted the electronic conduction of these slags as semiconduction, where the different oxidation states of the transition metal cations would act as ion pairs. For the TiO_2-SiO_2-Al_2O_3-MgO-CaO slags under study, EIS measurements were used to determine the temperature dependence of electrolyte resistance. The electrolyte resistance decreased with increasing temperature suggesting that the slag may act as a semiconductor. This is consistent with expectations for a melt containing TiO_2, a known semiconductor.[11] Furthermore, semiconducting behaviour has been seen in most of the Earth's mantle minerals,[27] including ferrous and titanate melts.[3,11,13]

The electronic conduction in many solid metal oxides has been proven polaronic in nature.[27] Recently, Barati and Coley[13] explained the electronic contribution to the mixed conduction of FeO_x−SiO_2−CaO slags with a diffusion-assisted charge transfer model. Briefly, the distance between the ferrous and ferric ions has to be sufficiently short to activate the tunnelling of electrons through the ion pair. The short-range electron-lattice interaction derived by this hopping mechanism between low- to high-valence ions is commonly referred to as small polaron. This model was also used by Hu et al.[3] to explain the electrical conductivity values for TiO_2−Ti_2O_3−FeO−SiO_2−Al_2O_3−MgO-CaO high titania slags. In order to test this theory in TiO_2-SiO_2-Al_2O_3-MgO-CaO slags, the dependence of the transference numbers on oxygen potential, temperature, TiO_2 content and melt structure will be discussed in the following sections.

B. Effect of TiO_2 Content

It is known that the electrical conductivity of titanium containing slags is predominantly ionic.[28,29] However, in slags containing high concentrations of TiO_2 (> 70 wt pct) electronic conduction has been reported to dominate.[3] Slag A (33 wt pct TiO_2), Slag B (15 wt pct TiO_2) and Slag C (9 wt pct TiO_2) were used to quantify the effect of TiO_2 concentration during electrolysis on the electronic conduction of the Ti-bearing slags.

The electronic transference number of the different slags as a function of temperature ranged from 0.04 to 0.25, and was found to vary with temperature and slag composition, with t_e increasing as the TiO_2 concentration increased (Figure 3). Ducret et al.[7] reported a similar behaviour in the electronic transference numbers with the concentration of FeO in FeO-CaO-MgO-SiO_2 melts. Fried et al.[11] identified titanium's multivalence as

responsible for the increase in electronic conduction, facilitating charge hopping. As the concentration of titanium cations increases in the melt, the density of suitable neighbouring ions increases, and an increase in the electronic conduction is found as expected.

The effect of the titania content of the melt on the total electrical conductivity is more complex. An increase of the titania content does not necessarily correlate with an increase on the total electrical conductivity. Mori mapped the total electrical conductivity for FeO_x-TiO_2 melts at 1673 K,[30] and CaO-SiO_2-TiO_2 melts at 1693 K.[28] Mori observed an increase in the total electrical conductivity with increasing TiO_2 for the latter, whilst a decrease was observed for the former with TiO_2 concentration up to 40 wt pct. Such contradicting behaviour is associated to the complex relation of TiO_2 with the structure of these slags. This effect will be further explored in Section 3.5.

C. Effect of Temperature

The electronic transference number were measured as a function of composition and temperature between 1773 and 1933 K (Figure 3). Temperatures around T_{liq} were chosen to investigate the effect of multi-phase conditions on the transference numbers. For Slag C and Slag B, t_e decreased initially. This is common for measurements made at $T_{sol} < T < T_{liq}$ where the composition of the molten portion will change due to the coexistence of both solid and liquid phases. In that two phase region, the solid phase fraction decreases with increasing temperature, which facilitates ionic mobility. That increases the ionic transference number, and, consequently, decreases t_e. From there, the t_e increased with temperature since both slag compositions are above their T_{liq}. Such increase can be attributed to molten semiconduction, in particular, to small polaron hopping as it is a thermally activated process; however, the effect of temperature on the electronic transference number is known to be temperature insensitive above the liquidus temperature, provided the activation energies for
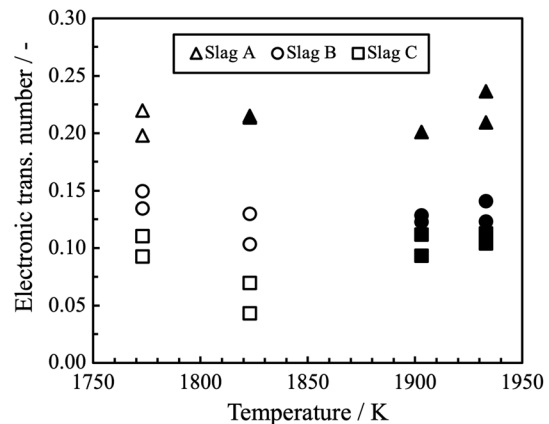
Fig. 3—Electronic transference number variation with temperature for Slag A, Slag B and Slag C at a fixed partial pressure of oxygen of 10^{-6} atm. Measurements below the predicted T_{liq} are presented with open symbols.

electronic conduction and ionic conduction are similar in value.[12] This is consistent with measurements made for Slag A. The insensitivity of t_e to temperature is most pronounced for Slag A since most of the SPC measurements for this slag composition were above its liquidus temperature (closed symbols in Figure 3). Sokhanvaran et al.[6] associated the increase of the electronic transference numbers to an increase in the disassociation of a cryolite-silica melt at temperatures above the T_{liq} that leads to an increase in the multi-valent anions. In all cases, it was found that the total electrical resistance (as measured by EIS) decreased as a function of increasing temperature. Whilst the intrinsic electrical resistivity could not be determined (due to the differences in cell geometry between measurements), the decrease in resistance as a function of temperature indicates that these melts behave as semi-conductors in agreement with other TiO_2-SiO_2-Al_2O_3-MgO-CaO slags[31] and many other molten oxide systems.[9]

D. Effect of Oxygen Potential

The partial pressure of oxygen (P_{O_2}) is known to influence the ratio of the different valences of the transition metal ions present in the slag. Three different gas atmospheres were used to study the effect of the partial pressure of oxygen on the electronic conduction of Slag A. From 1823 K to 1933 K, the t_e increased as the partial pressure of oxygen decreased (Figure 4). As all of these measurements were done at temperatures above the T_{liq}, in this molten state, the electronic transference number dependency on the P_{O_2} is an indication of a semiconducting mechanism.[31] According to the model proposed by Barati and Coley,[13] the electronic conduction should reach a maximum when the ratio of ions with different oxidation states (e.g., Ti^{4+}, Ti^{3+}) reaches unity, as this would provide the highest likelihood that two ions with different oxidation states will be close enough for charge to transfer between these ions. Then, provided that the ionic conductivity is not affected, this would in turn result in the t_e increasing. In titanium bearing slags, the distribution amongst Ti^{4+}, Ti^{3+}, and Ti^{2+} valence states
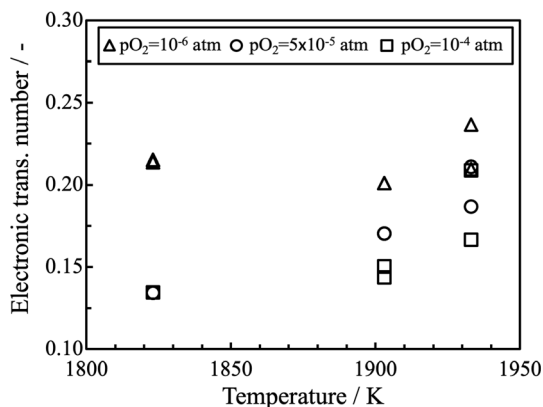
depends on slag composition, temperatures and oxygen partial pressures. Tranell et al.[32] investigated the redox behaviour of titanium in CaO-SiO_2-TiO_x slags with up to 52.3 wt pct TiO_2, and found that most reduced titanium was in Ti^{3+} valence in the melt at oxygen partial pressures between 10^{-12} and 10^{-7} atm. In the present study, similar experimental conditions were used, and hence all reduced titanium in the slag is reported as Ti^{3+}.

The effect of the temperature and P_{O_2} on the Ti^{3+} / Ti^{4+} ratio were predicted for Slag A using FactSage. FactSage's Equilib module[18] performs a Gibbs energy minimization routine to calculate the concentration of the chemical species present when the system reaches chemical equilibrium at constant pressure and temperature. The thermodynamic calculations showed that the ratio between Ti^{3+} and Ti^{4+} increases with increasing temperature (Figure 5). This is consistent with the endothermic character of the reduction of TiO_2 to Ti_2O_3.[33] Ti^{4+} is the most predominant titanium oxidation state in the melt. This is consistent with thermodynamic predictions in the temperature range studied, where the oxidation of Ti_2O_3 to TiO_2 is thermodynamically favoured.[34] The concentration of Ti^{3+} increases with decreasing oxygen partial pressure, as lower oxygen potentials favours the reduction of Ti^{4+}.[32]

The ability of electrons to act as charge carriers depends on the availability of unoccupied electronic states. Ti^{3+} has been found to increase electronic conductivity by creating holes in the valence band in crystalline titanium sesquioxide.[35] Consistent with the work of others,[13] here we find that the measured electronic transference number, t_e, increases when the ratio multi-valent ions (in this case the Ti^{3+} /Ti^{4+} ratio) increases (Figure 6). Whilst there is limited data for Slag B and C, based on the mechanism proposed by Barati and Coley,[13] it would be expected that if these slags contained higher Ti^{3+} /Ti^{4+} ratios, the electronic transference number would also increase to similar levels found in Slag A at high Ti^{3+} /Ti^{4+} ratios. Since electron mobility is usually much higher than ionic mobility, it is

Fig. 4—Electronic transference number as a function of temperature at different partial pressures of oxygen for Slag A.
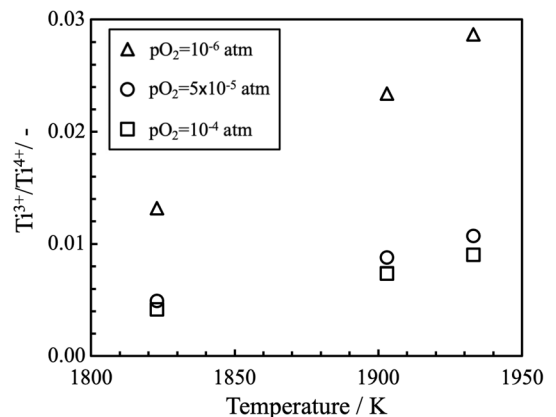
Fig. 5—The predicted equilibrium speciation ratio, between Ti^{3+} and Ti^{4+} as a function of temperature for various partial pressures of oxygen for Slag A.

speculated that even a small quantity of mixed valence is sufficient to generate electronic conductivity. Whilst Figure 6 shows a correlation between the Ti^{3+}/Ti^{4+} ratio and the electronic transference number, a two-parameter regression using both the wt pct TiO_2 and Ti^{3+}/Ti^{4+} ratio was found to be statistically more significant (F-statistic = 44.7) than a single factor regression (F-statistic = 24.4) using only the Ti^{3+}/Ti^{4+} ratio. Furthermore, incorporating T and pO_2 into the regression did not improve the F-statistic. Whilst this analysis suggests that the most important factors controlling the electronic transference number are the Ti content and Ti^{3+}/Ti^{4+} ratio, without a physico-chemical model describing the electronic properties of the melt, it is too early to draw strong conclusions from this data.

E. Effect of Melt Structure

Initial attempts to explain the conductive mechanism of molten oxides were derived from the theory of electric conduction in ionic liquids.[36,37] This approach, even though successful to explain the behaviour in molten salts, fails in its application to complex molten silicates because it does not consider short-range ordering.[25] Mysen[38] and, more recently, Min and Tsukihashi[25] reviewed the XRD, nuclear magnetic resonance and raman spectroscopy literature and found that a 3-dimensional interconnected network of tetrahedral silicate anionic units was consistent within silicate slags. The effect of structural changes (e.g., phase transitions) on the total electrical conductivity on solid silicate minerals has been studied before.[27] As free ions in the slag are the only ionic charge carriers,[10] ionic conduction strongly depends upon structure.[25] The location of metal cations in the silica network at their substitutional Si sites or at interstitial sites in the free volume affects the degree of polymerisation and, hence, the transport properties of silicate melts.[14,38]

The effect of the melt structure is expected to prevail for the ionic conduction as it is achieved by the migration of ions.[25] The Nernst-Einstein equation defines the total electrical conductivity in an ionic

Fig. 6—Electronic transference number variation with the predicted equilibrium speciation ratio, between Ti^{3+} and Ti^{4+}, measured for Slag A, Slag B and Slag C above their predicted T_{liq}.

conductor as proportional to the number and mobility of charge carriers.[27] It is then expected that the slag depolymerization will positively influence the ionic conduction facilitating the movement of ions through the melt. The optical basicity, Λ, is a common metric used in process metallurgy to measure the degree of depolymerization of silicate systems.[14] In oxide networks, it indicates the proportion of basic oxides. In more acidic slags (i.e., higher fraction of the network-forming ions) the degree of polymerization is higher. Λ is a concept derived from the bonding characteristics of the Lewis acid-base theory,[39] and it has been experimentally correlated to the position of equilibrium for redox reaction within the melt[39] and to parameters such as viscosity in ironmaking slags.[40] The optical basicity calculated for the different slag compositions was corrected (see Λ_{corr} in Table I) to account for the numbers of Ca^{2+} cations needed to charge balance the Al^{3+} incorporated into the silicate network.[14] Slag A has the lowest Λ_{corr}, so it should present a larger opposition to ionic diffusion than Slag B and Slag C. This is consistent with Slag A having the highest t_e (see Figure 3). However, the values of Λ_{corr} are very close for all slag compositions, indicating a similar degree of polymerization and of ionic mobility. Additionally, above 1773 K, TiO_2 does not have any significant effect on viscosity, with values less than 0.5 Pa.s.[41,42] The low and almost constant viscosity along with the small deviation in Λ_{corr} indicates that the influence of structure on the ionic conduction for the temperatures and composition measured will be minor.

With regards to the slag chemistry, the effect is more prevalent on the electronic conduction due to the electronic conduction mechanism of these transition metal cation-bearing slags.[25] As explained before, hopping conduction requires neighbouring ions of different valence for the charge transfer to occur.[12] Previous research[32,43] has shown that the amount of Ti^{3+} in the melt increased with the decreasing basicity when the temperature and oxygen partial pressure were kept constant. A less basic system is more polymerized, it contains fewer free oxygen anions, and more Ti^{3+}.[39] This is consistent with the trend observed with reducing atmospheres in Section 3.4. The Ti^{3+}/Ti^{4+} ratio was predicted using FactSage for Slag A, Slag B and Slag C at a fixed partial pressure of oxygen of 10^{-6} atm. This ratio was found to increase as a function of temperature (Figure 7) as discussed in the previous section.

The predicted fraction of Ti^{3+} changed slightly with increasing TiO_2 concentrations from 9 (Slag C) up to 33 wt pct (Slag A) (Figure 7). The values agree with those reported by Tranell et al.[32] for the amount of TiO_2 in the melt. However, it is worth noting that Tranell et al.[32] observed a more complex relation between the amount of TiO_2 in the melt and the Ti^{3+}/Ti^{4+} ratio. For concentrations up to 14 wt pct in $CaO-SiO_2-TiO_x$, an increase of TiO_2 lead to a decreased in the ratio, whilst the trend was reversed if the concentration of TiO_2 was increased up to 50 wt pct. This behaviour can be related to a change of the oxygen coordination state

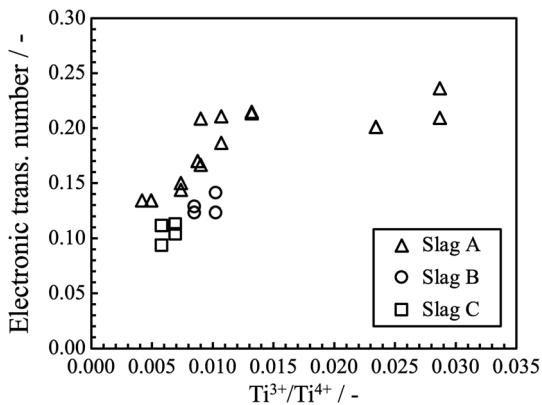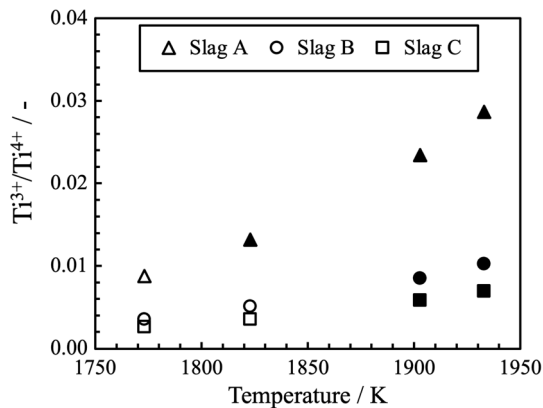Fig. 7—The predicted equilibrium speciation ratio, between Ti^{3+} and Ti^{4+}, variation with temperature and slag composition at a fixed partial pressure of oxygen of 10^{-6} atm. Data measured below the predicted T_{liq} are presented with open symbols.

of Ti^{4+} with TiO_2 content.[38] The contradictory effect of TiO_2 content on the total electrical conductivity of titania containing slags without silica[30] and titania containing slags with silica[28] may be also attributed to this complex relationship. Accordingly, incorporating the actual structural changes associated with TiO_2 addition is a hard task with on-going research efforts.[44]

IV. CONCLUSIONS

The mixed conduction mechanism of molten TiO_2-SiO_2-Al_2O_3-MgO-CaO slags was assessed using EIS and SPC measurements, where the contribution of the ionic and electronic charge carriers were quantified as temperature, oxygen partial pressure, and electrolyte composition were varied. The main conclusions are summarized as follows:

1. Across all the temperatures studied, the t_e increased as TiO_2 concentration increased from 9 to 33 wt pct. Further experiments must be done before extrapolating to other concentrations as the oxygen coordination state of Ti^{4+} has been reported to change with TiO_2 content.
2. The effect of temperature on the t_e was minor for the range of temperatures studied above T_{liq}.
3. Decreasing the oxygen potential from 10^{-4} to 10^{-6} atm increased the partition between Ti^{3+} and Ti^{4+}, and increased the t_e. The oxygen partial pressure dependence of t_e is an indication of a semiconducting mechanism in the molten slag.
4. The influence of structure in the ionic conduction was minor as the degree of depolymerization and the viscosity for the slags studied has been reported nearly constant within the temperature and composition range investigated.

The electronic transference number of the different slags ranged from 0.04 to 0.25 and was found to vary mainly with Ti^{3+}/Ti^{4+} ratio and total titanium content. This is consistent with the diffusion-assisted charge transfer model recently used to explain electronic conduction on

molten FeO_x bearing slags. The understanding gained about the conductive mechanism of the slag in relation with its physical-chemical properties and the extent to which it is affected by changing the experimental processing conditions provides valuable information that is required to optimize the recycling of the slag.

CONFLICT OF INTEREST

The authors declare that they have no conflict of interest.

OPEN ACCESS

REFERENCES

1. C. Bataille, M. Ahman, K. Neuhoff, L.J. Nilsson, M. Fischedick, S. Lechtenbohmer, B. Solano-Rodriquez, A. Denis-Ryan, S. Stiebert, H. Waisman, O. Sartor, and S. Rahbar: *J. Clean. Prod.*, 2018, vol. 187, pp. 960–93.
2. S. Martin-Treceno, N. Weaver, A. Allanore, C.M. Bishop, A.T. Marshall, and M.J. Watson: *Electrochim. Acta*, 2020, vol. 354, p. 136619.
3. K. Hu, X. Lv, W. Yu, Z. Yan, W. Lv, and S. Li: *Metall. Mater. Trans. B*, 2019, vol. 50B, pp. 2982–92.
4. A.E. Gheribi, A. Serva, M. Salanne, K. Machado, D. Zanghi, C. Bessada, and P. Chartrand: *ACS Omega*, 2019, vol. 4, pp. 8022–30.
5. S. Poizeau, and D.R. Sadoway: in *Light Metals 2011 - TMS 2011 Annual Meeting and Exhibition, February 27, 2011 - March 3*, Minerals, Metals and Materials Society, TMS Light Metals, 2011, pp. 387–92.

6. S. Sokhanvaran, S. Thomas, and M. Barati: *Electrochim. Acta*, 2012, vol. 66, pp. 239–44.
7. A. Ducret, D. Khetpal, and D.R. Sadoway: *ECS Proc. Vol.*, 2002, vol. 19, pp. 347–53.
8. J. Van Der Colf, and D.D. Howat: *J. S. Afr. Inst. Min. Metall.*, 1979, vol. 79, pp. 255–63.
9. A.E. Van Arkel, E.A. Flood, and N.F.H. Bright: *Can. J. Chem.*, 1953, vol. 31, pp. 1009–19.
10. S. Wang, G. Li, T. Lou, and Z. Sui: *ISIJ Int.*, 1999, vol. 39, pp. 1116–19.
11. N.A. Fried, K.G. Rhoads, and D.R. Sadoway: *Electrochim. Acta*, 2001, vol. 46, pp. 3351–58.
12. M. Barati, and K.S. Coley: *Metall. Mater. Trans. B*, 2006, vol. 37B, pp. 41–49.
13. M. Barati, and K.S. Coley: *Metall. Mater. Trans. B*, 2006, vol. 37B, pp. 51–60.
14. K.C. Mills: *ISIJ Int.*, 1993, vol. 33, pp. 148–55.
15. B.R. Nakanishi, and A. Allanore: *J. Electrochem. Soc.*, 2017, vol. 164, pp. E460–71.
16. H. Kahlert: *Reference Electrodes*, Springer, Berlin, 2010, pp. 291–308.
17. A. Caldwell, E. Lai, A. Gmitter, and A. Allanore: *Electrochim. Acta*, 2016, vol. 219, pp. 178–86.
18. C. Bale, E. Belisle, P. Chartrand, S. Decterov, G. Eriksson, A. Gheribi, K. Hack, I.-H. Jung, Y.-B. Kang, J. Melancon, A. Pelton, S. Petersen, C. Robelin, J. Sangster, P. Spencer, and M.-A.V. Ende: *Calphad,* 2016, vol. 54, pp. 35–53.
19. A.J. Bard, and L.R. Faulkner: *Electrochemical Methods: Fundamentals and Applications*, 2nd edn., Wiley, New York, 2001.
20. J.W. Arblaster, and J. Matthey: *Technol. Rev.*, 2016, vol. 60, pp. 4–11.
21. I. Olsen, R. Koksbang, and E. Skou: *Electrochim. Acta*, 1995, vol. 40, pp. 1701–06.
22. M. Pomeroy, G. Brown, M. Barati, and K.S. Coley: *High Temp. Mater. Proc.*, 2012, vol. 31, pp. 231–36.
23. J.L. Cann: *Master's Thesis*, Massachusetts Institute of Technology, Cambridge, MA, 2017.
24. S.K. Ratkje, H. Rajabu, and T. Førland: *Electrochim. Acta*, 1993, vol. 38, pp. 415–23.
25. D.J. Min and F. Tsukihashi: *Met. Mater. Int.*, 2017, vol. 23, pp. 1–19.
26. N. Mott: *J. Non-Cryst. Solids*, 1972, vol. 8–10, pp. 1–18.
27. T. Yoshino: *Surv. Geophys.*, 2010, vol. 31, pp. 163–206.
28. K. Mori: *Tetsu-to-Hagane*, 1960, vol. 46, pp. 134–40.
29. K.C. Mills, and B.J. Keene: *Int. Mater. Rev.*, 1987, vol. 32, pp. 1–20.
30. K. Mori: *Tetsu-to-Hagane*, 1956, vol. 42, pp. 1024–29.
31. J. Van Der Colf, and D.D. Howat: *J. S. Afr. Inst. Min. Metall.*, 1979, vol. 79, pp. 327–33.
32. G. Tranell, O. Ostrovski, and S. Jahanshahi: *Metall. Mater. Trans. B*, 2002, vol. 33B, pp. 61–67.
33. H.D. Schreiber: *J. Non-Cryst. Solids*, 1986, vol. 84, pp. 129–41.
34. L. Zhang, L. Zhang, M. Wang, G. Li, and Z. Sui: *ISIJ Int.*, 2006, vol. 46, pp. 458–65.
35. J. Yahia, and H.P.R. Frederikse: *Phys. Rev.*, 1961, vol. 123, pp. 1257–61.
36. J.C. Ghosh: *J. Chem. Soc. Trans.*, 1918, 113, pp. 449–58.
37. J.C. Dyre: *J. Appl. Phys.*, 1988, vol. 64, pp. 2456–68.
38. B.O. Mysen: *Earth-Sci. Rev.*, 1990, vol. 27, pp. 281–65.
39. J.A. Duffy: *Geochim. Cosmochim. Acta* 1993, vol. 57, pp. 3961–70.
40. K.C. Mills, and S. Sridhar: *Ironmak. Steelmak.*, 1999, vol. 26, pp. 262–68.
41. Slag Atlas, Verlag Stahleisen, Düsseldorf, 2nd ed., 1995.
42. J.L. Liao, J. Li, X.D. Wang, and Z.T. Zhang: Ironmak. Steelmak., 2012, vol. 39, pp. 133–39.
43. J. Li, Z. Zhang, M. Zhang, M. Guo, and X. Wang: *Steel Res. Int.*, 2011, vol. 82, pp. 607–14.
44. G.H. Zhang, K.C. Chou, and J.L. Zhang: *Ironmak. Steelmak.*, 2014, vol. 41, pp. 47–50.